

RESEARCH ARTICLE

Quadcopter Precision Landing on Moving Targets via Disturbance Observer-Based Controller and Autonomous Landing Planner

NGUYEN XUAN-MUNG¹, (Member, IEEE), NGOC PHI NGUYEN¹, TAN NGUYEN², DINH BA PHAM³, MAI THE VU⁴, HA LE NHU NGOC THANH⁵, AND SUNG KYUNG HONG^{1,6}

¹Department of Aerospace Engineering, Sejong University, Seoul 05006, South Korea

²Department of Technology, Dong Nai Technology University, Bien Hoa 810000, Vietnam

³Department of Mechanical Engineering, Vietnam Maritime University, Haiphong 180000, Vietnam

⁴School of Intelligent Mechatronics Engineering, Sejong University, Seoul 05006, South Korea

⁵Department of Mechatronics Engineering, Ho Chi Minh City University of Technology and Education, Ho Chi Minh City 71307, Vietnam

⁶Department of Convergence Engineering for Intelligent Drone, Sejong University, Seoul 05006, South Korea

Corresponding authors: Nguyen Xuan-Mung (xuanmung@sejong.ac.kr) and Sung Kyung Hong (skhong@sejong.ac.kr)

This work was supported in part by the Ministry of Science and ICT (MSIT), South Korea, through the Information Technology Research Center (ITRC) Support Program supervised by the Institute for Information & Communications Technology Planning & Evaluation (IITP) under Grant IITP-2022-2018-0-01423; and in part by the Basic Science Research Program through the National Research Foundation of Korea (NRF) funded by the Ministry of Education under Grant 2020R1A6A1A03038540.

ABSTRACT Unmanned aerial vehicles, especially quadcopters, play key roles in many real-world applications and the related quadcopter autonomous control algorithms have attracted a great deal of attention. In this paper, we address the vision-based autonomous landing problem of a quadcopter on a ground moving target. Firstly, we propose a disturbance observer-based control algorithm, consisting of a nonlinear disturbance observer and robust altitude and attitude controllers. This algorithm is based on the quadcopter dynamics model, and its stability is strictly proved using Lyapunov's theory. Secondly, we develop an autonomous landing planner which we test for various landing scenarios to deliver improved reliability and accuracy of the landing mission. These theoretical studies are complemented by a numerical feasibility study, before demonstrating the effectiveness of our approach under actual flight conditions with an experimental quadcopter platform.


INDEX TERMS Autonomous vehicle, quadcopter, unmanned aerial vehicle, precision landing, moving target, disturbance observer, robust control, mission planning.

I. INTRODUCTION

In recent decades, quadcopter unmanned aerial vehicles (UAVs) have gained much appreciation in the community due to their various benefits over other UAVs, namely an ability for vertical takeoff and landing, high agility and maneuverability, compact size, and affordable cost [1]. Therefore, they have attracted a growing attention for various applications, including search and rescue, environmental exploration, surveillance, and aerial mappings [2]. In all these applications, landing the vehicle is an essential yet delicate

maneuver [3], with sensing limitations, external disturbances, and unknown landing surfaces posing the main challenges. The task is complicated even further if the landing target is in motion. Hence, the ability to reliably land a quadcopter autonomously on a moving platform remains a highly challenging but also rewarding topic as it promises a multitude of applications.

Positioning is one of the fundamental parameters that directly affect landing performance. While the global positioning system (GPS) is popular for outdoor positioning [4], it is considerably degraded in clustering environments such as cities with high buildings, narrow valleys, and forests. Furthermore, there is no GPS reception indoors or in caves.

The associate editor coordinating the review of this manuscript and approving it for publication was Cesar Briso .

To resolve these issues, many studies successfully employed other onboard sensors to provide alternative solutions to the positioning problem in GPS-denied environments [5]. The most commonly used onboard sensors include ultrasonic rangars, laser rangars, light detecting and ranging (Lidar) sensors, and visual cameras [6].

From among these approaches, visual cameras are highly suitable for precision landing missions as they can provide 3-dimensional (3D) or at least 2D information about the landing target's state [7]. In the past, two main approaches have been employed for vision-based autonomous quadcopter landing, namely image-based visual servoing [8] and position-based visual servoing (PBVS) [9], with the latter having several advantages considering that quadcopters are an underactuated system. As a result, PBVS has been utilized in many landing algorithms, including linear [10], [11] and nonlinear [12], [13] control techniques. However, all these studies tackled the landing problem for stationary platforms only and did not consider moving platforms.

Since many applications require quadcopters to be able to land on a mobile target, some studies have attempted to solve this problem. However, in [14] it was assumed that the target's velocity is known, which is not the case in most real-world applications. In [15], the PID control technique was used to land a quadcopter on a fast-moving ground vehicle, although the vehicle's position and velocity had to be determined from an attached smartphone's GPS information. Several other approaches that are based on the landing target's model have been presented in the literature [16], [17], [18], including approaches using control methods and data estimation algorithms [19], [20], [21], [22], [23]. However, most of these works used optical cameras operating in the visual part of the spectrum and are therefore unsuitable for dark environments, e.g., during nighttime or for applications in caves or tunnels. Moreover, most of these studies did not present any experimental verifications of the proposed algorithms. Meanwhile, the problem of reliably landing a quadcopter on a moving target remains unresolved for a wide range of real-world applications and solutions are desperately needed.

In an effort to provide such a solution, we propose the following approach to land a quadcopter precisely on a ground moving target in the presence of external disturbances. The main contributions of this work are fourfold:

(i) A novel disturbance observer-based (DOB) control algorithm is proposed to deal with the robust altitude and attitude tracking control problems of quadcopters in disturbed flight conditions. The stability of the closed-loop system is strictly proved using Lyapunov's theory. Our proposed controller only requires tuning of a few parameters and is robust against external disturbances, which are omnipresent and can severely degrade the low-altitude flight performance of quadcopters [24], [25], especially when close to the landing pad.

(ii) A new autonomous landing planner is developed. By testing several landing scenarios, we ensure that the planner can execute the mission safely and precisely. More

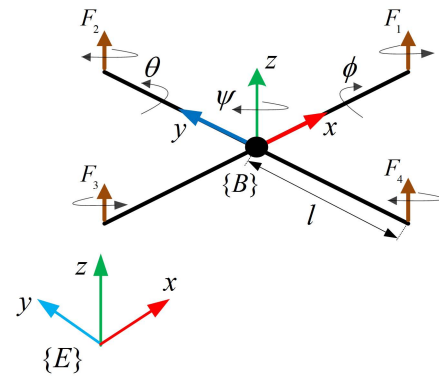


FIGURE 1. A typical quadcopter configuration.

specifically, our planner achieves a higher landing success rate, and even when the UAV cannot be safely landed on the moving target, it will deviate the vehicle and safely land it in an alternative landing location.

(iii) We employ an infrared (IR) camera for the landing target detection and state estimation which ensures that our approach remains fully functional also in dark environments, while making it cost efficient and simple to operate as it requires only one small, lightweight IR beacon that can be easily attached to any landing platform. This is highly beneficial from a practical point of view as many missions require quadcopters to be able to operate in the dark (e.g., disaster monitoring, surveillance, search and rescue) and land autonomously on moving targets (e.g., ship decks or trucks).

(iv) Unlike many existing studies, who only validated their algorithms through numerical simulations, we conducted several experiments with realistic flight conditions to demonstrate the effectiveness of our method. The movement of a ground vehicle is simulated by attaching a landing platform onto a rover. To the best of our knowledge, only few studies [26], [27], [28] have been able to verify their approach experimentally and we highlight the advantages of our method in a direct comparison (Table 1).

The remainder of this paper is organized as follows. Section II presents preliminaries. The proposed DOB robust controller and the autonomous landing planner are described in Section III. Experimental setups and results are presented in Section IV, and conclusions are given in Section V.

II. QUADCOPTER DYNAMICS AND PROBLEM STATEMENT

A widely used configuration of a quadcopter is depicted in Figure 1. With four motors and four propellers, the vehicle can generate forces $F_i (i = 1, \dots, 4)$ that manipulate the vehicle's rigid body through control inputs, including the thrust force (u_1) and torques ($u_2, u_3,$ and u_4):

$$\begin{cases} u_1 = F_1 + F_2 + F_3 + F_4 \\ u_2 = L(F_2 - F_4) \\ u_3 = L(F_3 - F_1) \\ u_4 = c_d(-F_1 + F_2 - F_3 + F_4) \end{cases} \quad (1)$$

TABLE 1. Comparing our proposed work and the most related works in the literature [26], [27].

Comparison Criteria	[26]	[27]	[28]	Our Work	Merit
Landing (altitude and attitude) controller	PID	P-P	Low complexity controller	Proposed DOB controller	Improved Reliability Our work is theoretically and practically reliable for quadcopter landing on mobile targets in the presence of considerable external disturbances.
Maximum speed of the moving target	0.4 m/s	0.8 m/s	0.5 m/s	2 m/s	Higher Realism The large speed of our landing target provides a more realistic approximation of the landing target's motion, thus ensuring the applicability of our work to real-world applications.
Camera system	IR camera	Visual spectrum camera	Visual spectrum camera	IR camera	Multifunction Our solution remains functional even in low-light or dark environments.
Landing error	35 cm	- - -	10 cm	18.6 cm	Improved Accuracy Our approach allows quadcopters to achieve missions requiring high landing accuracy.

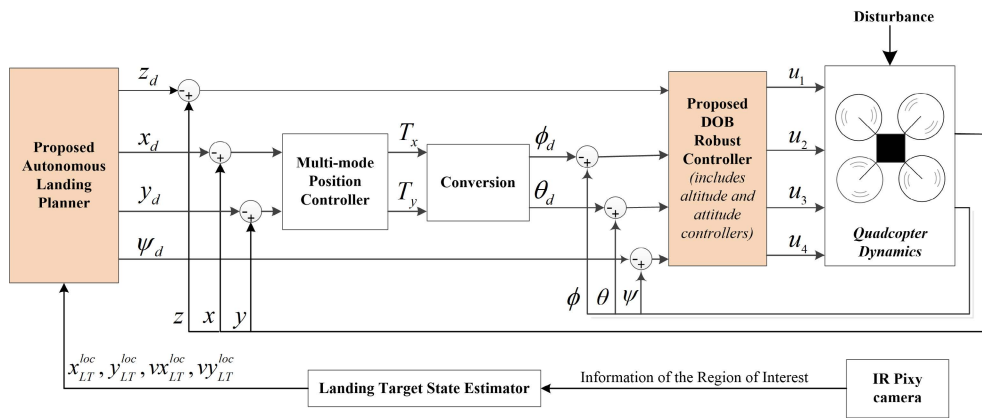


FIGURE 2. Block diagram of the proposed algorithms, including a DOB controller and a autonomous landing planner, in the whole control system of the quadcopter.

where L is the quadcopter's arm length; c_d the force-to-torque coefficient; and g the gravitational acceleration.

The quadcopter dynamics was described and verified in various existing studies [29], [30], [31]. Its horizontal translational dynamics model is expressed as

$$\begin{cases} \ddot{x} = \frac{1}{m}(\cos\phi\sin\theta\cos\psi + \sin\phi\sin\psi)u_1 \\ \ddot{y} = \frac{1}{m}(\cos\phi\sin\theta\sin\psi - \sin\phi\cos\psi)u_1 \end{cases} \quad (2)$$

and its vertical and rotary dynamics are described as

$$\begin{cases} \ddot{z} = -g + \frac{1}{m}(\cos\phi\cos\theta)u_1 + d_1 \\ \ddot{\phi} = \frac{J_y - J_z}{J_x}\dot{\theta}\dot{\psi} + \frac{1}{J_x}u_2 + d_2 \\ \ddot{\theta} = \frac{J_z - J_x}{J_y}\dot{\psi}\dot{\phi} + \frac{1}{J_y}u_3 + d_3 \\ \ddot{\psi} = \frac{J_x - J_y}{J_z}\dot{\phi}\dot{\theta} + \frac{1}{J_z}u_4 + d_4 \end{cases} \quad (3)$$

with x, y being the position, z the altitude, and ϕ, θ, ψ the attitude (in the inertial coordinate $\{E\}$); m denotes the mass; J_x, J_y , and J_z represent the momentum of inertia about the x, y , and z axes, respectively; $d = [d_1, d_2, d_3, d_4]^T$ is the disturbance vector.

It is worth noting that the quadcopter's dynamics are separated into horizontal translational terms in (2) and the other terms in (3) because of the following reasons.

(i) As per (2), the dynamics of the position x , and y are dependent to the attitude ϕ, θ, ψ and the control input u_1 . Therefore, we can manipulate the vehicle's position by controlling its altitude and attitude in (3).

(ii) In this paper, we are going to focus on proposing a disturbance observer-based controller to stabilize the vertical and rotary dynamics (3).

Let $\xi = [z, \phi, \theta, \psi]^T$, $u = [u_1, u_2, u_3, u_4]^T$, $f = [-g, \frac{J_y - J_z}{J_x}\dot{\theta}\dot{\psi}, \frac{J_z - J_x}{J_y}\dot{\psi}\dot{\phi}, \frac{J_x - J_y}{J_z}\dot{\phi}\dot{\theta}]^T$, and $B = \text{diag}(\frac{1}{m}\cos\phi\cos\theta, \frac{1}{J_x}, \frac{1}{J_y}, \frac{1}{J_z})$. Then, (3) becomes

$$\ddot{\xi} = f + Bu + d \quad (4)$$

In the following sections, we are going to present a disturbance observer-based controller, u , and a landing planner (Figure 2), which allow the quadcopter to land precisely on a moving target with a time-varying position of (x_d, y_d) . In this paper, we use a mini-rover as the landing target, whose car-like model is illustrated in Figure 3 and kinematics is described as follows [32].

$$\begin{cases} \dot{x}_r = v\cos\theta_r \\ \dot{y}_r = v\sin\theta_r \\ \dot{\theta}_r = \frac{v}{L_r}\tan\delta_r \end{cases} \quad (5)$$

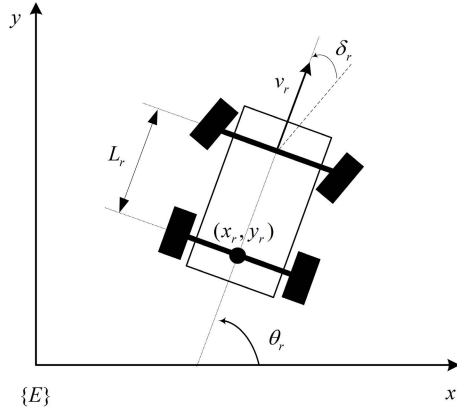


FIGURE 3. The car-like model of the mini-rover, which is used as a moving landing target in this study.

where x_r and y_r denote the position of the characteristic point located midway of the rear wheels, θ_r the heading angle, and δ_r the steering angle of the rover. Before moving forward, the following assumption and lemma are introduced.

Assumption 1: The disturbance d and its time-derivative are bounded, i.e., the followings hold: $\|d\| \leq d_L$ and $\|\dot{d}\| \leq \delta_L$, where d_L and δ_L are unknown positive constants.

Lemma 1 [33]: Consider a system $\dot{x} = h(x) + u + d(t, x)$ where $x \in \mathbb{R}^n$, $h(x)$ is a vector of smooth functions, and u is the control signal, then, the following disturbance observer is introduced:

$$\begin{cases} \dot{\hat{d}}(t, x) = \mu + \eta(x) \\ \dot{\mu} = -L(x)\mu - L(x)[h(x) + u + \eta(x)] \end{cases} \quad (6)$$

where $L(x) = \partial\eta(x)/\partial x$ denotes the observer gain, $\eta(x)$ is selected in such way that $L(x)$ be a positive-definite gain matrix for all $x \in \mathbb{R}^n$. The disturbance observer (6) ensures that the observation error $\tilde{d}(t, x) = d(t, x) - \hat{d}(t, x)$ exponentially tends to a residual set containing the zero whose radius is adjustable by tuning the function $\eta(x)$. If $d_L = 0$, the observer error exponentially tends to the origin.

III. MAIN RESULTS

A. DISTURBANCE OBSERVER-BASED CONTROLLER

Let $\xi_{sp} = [z_{sp}, \phi_{sp}, \theta_{sp}, \psi_{sp}]^T$ be the control setpoint, then the tracking error can be defined as:

$$e_\xi = \xi - \xi_{sp} \quad (7)$$

Then, we have the followings:

$$\dot{e}_\xi = \dot{\xi} - \dot{\xi}_{sp} \quad (8)$$

and

$$\ddot{e}_\xi = \ddot{\xi} - \ddot{\xi}_{sp} \quad (9)$$

From (4) and (9), we have the dynamics of the tracking error as

$$\ddot{e}_\xi = f + Bu + d - \ddot{\xi}_{sp} \quad (10)$$

Let (10) be rewritten as

$$\ddot{e}_\xi = v \quad (11)$$

with v being a virtual control input,

$$v = f + Bu + d - \ddot{\xi}_{sp} \quad (12)$$

The selection of virtual input v is based on the stability of the tracking error dynamics. Thus, by defining the following variable

$$\sigma = \dot{e}_\xi + \Lambda e_\xi (e_\xi^T e_\xi + 1)^{-\frac{1}{2}} \quad (13)$$

a control law is proposed as

$$v = -K\sigma = -K\dot{e}_\xi - K\Lambda e_\xi (e_\xi^T e_\xi + 1)^{-\frac{1}{2}} \quad (14)$$

where K and Λ are controller's gains. By substituting (15) into (12), the following DOB controller is obtained

$$u = B^{-1}[-K\dot{e}_\xi - K\Lambda e_\xi (e_\xi^T e_\xi + 1)^{-\frac{1}{2}} - \zeta - f + \ddot{\xi}_{sp} - \hat{d}] \quad (15)$$

where,

$$\zeta = \Lambda \dot{e}_\xi (e_\xi^T e_\xi + 1)^{-\frac{3}{2}} \quad (16)$$

$$\hat{d} = \mu + \Gamma\sigma \quad (17)$$

$$\dot{\mu} = -\Gamma\mu - \Gamma[f - \ddot{\xi}_{sp} + Bu + \zeta + \Gamma\sigma] \quad (18)$$

where \hat{d} is the estimate of the disturbance and Γ is the observer gain. Thus, the time-derivative of (13) along (10) gives:

$$\begin{aligned} \dot{\sigma} &= \ddot{e}_\xi + \Lambda \dot{e}_\xi (e_\xi^T e_\xi + 1)^{-\frac{3}{2}} \\ &= f + Bu + d - \ddot{\xi}_{sp} + \Lambda \dot{e}_\xi (e_\xi^T e_\xi + 1)^{-\frac{3}{2}} \\ &= -K\dot{e}_\xi - K\Lambda e_\xi (e_\xi^T e_\xi + 1)^{-\frac{1}{2}} + \tilde{d} \end{aligned} \quad (19)$$

where, $\tilde{d} = d - \hat{d}$.

From (17)-(18), one can obtain:

$$\dot{\tilde{d}} = \dot{d} + \Gamma\mu + \Gamma[f - \ddot{\xi}_{sp} + Bu + \zeta + \Gamma\sigma] \quad (20)$$

which can be simplified as

$$\dot{\tilde{d}} = \dot{d} - \Gamma\tilde{d} \quad (21)$$

The stability of the closed-loop system with the proposed disturbance observer-based controller is summarized in the following theorem.

Theorem 1: For a given time-varying setpoint ξ_{sp} , the control law (15), based on the observer in (17) and (18), asymptotically stabilize the quadcopter system (4), i.e., the tracking error, e_ξ , is forced to zero in a finite time.

Proof: Consider the following Lyapunov function candidate:

$$V = (e_\xi^T e_\xi + 1)^{\frac{1}{2}} - 1 + \frac{1}{2}\sigma^T \sigma + \frac{1}{2}\tilde{d}^T \tilde{d} \quad (22)$$

Then, the derivative of V gives

$$\dot{V} = (e_\xi^T e_\xi + 1)^{-\frac{1}{2}} e_\xi^T \dot{e}_\xi + \sigma^T \dot{\sigma} + \frac{1}{2}\tilde{d}^T \dot{\tilde{d}} + \frac{1}{2}\dot{\tilde{d}}^T \tilde{d} \quad (23)$$

Substituting (19) and (21) into (23) yields

$$\dot{V} = (e_{\xi}^T e_{\xi} + 1)^{-\frac{1}{2}} e_{\xi}^T \sigma - (e_{\xi}^T e_{\xi} + 1)^{-\frac{1}{2}} e_{\xi}^T \Lambda e_{\xi} (e_{\xi}^T e_{\xi} + 1)^{-\frac{1}{2}} - \sigma^T K \sigma + \sigma^T \tilde{d} + \dot{\tilde{d}} - \tilde{d}^T (\Gamma^T + \Gamma) \tilde{d} / 2 \quad (24)$$

Considering $\tilde{d}^T (\Gamma^T + \Gamma) \tilde{d} / 2 \geq \gamma_0 \tilde{d}^T \tilde{d}$ and the fact that $ab \leq \epsilon a^2 + b^2 / (4\epsilon), \forall \epsilon > 0$, we have

$$\begin{aligned} \dot{V} &\leq -(\Lambda - \epsilon) e_{\xi}^T e_{\xi} (e_{\xi}^T e_{\xi} + 1)^{-1} - (K - \frac{1}{4\epsilon} - \epsilon) \sigma^T \sigma \\ &\quad - (\Gamma - \frac{1}{4\epsilon} - \epsilon) \tilde{d}^T \tilde{d} + \frac{1}{4\epsilon} \| \dot{\tilde{d}} \|^2 \\ &\leq -\lambda \| \Omega \|^2 + \varepsilon \end{aligned} \quad (25)$$

where $\lambda := \min(\lambda_e, \lambda_{\sigma}, \lambda_d)$, with $\lambda_e := \Lambda - \epsilon > 0, \lambda_{\sigma} := K - \frac{1}{4\epsilon} - \epsilon > 0$, and $\lambda_d := \gamma_0 - \frac{1}{4\epsilon} - \epsilon > 0; \Omega := [e_{\xi}^T (e_{\xi}^T e_{\xi} + 1)^{-\frac{1}{2}}, \sigma^T, \tilde{d}^T]^T$; and $\varepsilon := \sup_{t \geq 0} (\frac{1}{4\epsilon} \| \dot{\tilde{d}} \|^2)$.

Following the comparison principle in [35], inequality (25) indicates the closed-loop system is uniformly ultimately bounded, and the tracking error converges to a small neighborhood of the origin. This completes the proof.

Remark 1: The larger Λ , the faster the altitude and attitude tracking errors converge to zero. However, care must be taken when choosing Λ as large values can cause the chattering phenomenon which increases system vibration and shortens the actuators' span. Furthermore, the convergence speed of σ is proportional to K . In our experiments, we found that Λ ranged from 0.8 to 1.2, while K was about 10 times larger than Λ . However, these ranges may depend on the type of quadcopter system and need to be tuned carefully by evaluating the system performance.

Remark 2: The larger Γ , the faster the disturbance estimation errors converge to zero. However, a large Γ makes the observer more sensitive to external disturbances which may cause jerks or even render the system unstable. Therefore, thorough evaluations using numerical simulations are recommended before applying the chosen observer gain to an experimental platform.

Remark 3: Equation $\sigma = 0$ plays the role of a sliding manifold [35], and the tracking error, e_{ξ} , is brought to this manifold and is maintained there by the controller (15).

B. LANDING PLANNER

We propose an autonomous landing planner to ensure that the landing mission executes safely and precisely. The planner activates a predefined procedure once the landing task has been triggered. The autonomous landing procedure is as follows:

- Step 1:* Start
- Step 2:* GPS-based horizontally approach the landing area.
- Step 3:* If the landing target (LT) is visible, vision-based horizontally approach the LT.
Else, jump to *Step 7*.
- Step 4:* If the vehicle and the LT are horizontally close, descend over the LT.
Else, jump to *Step 3*.
- Step 5:* If the LT is lost, jump to *Step 6*.

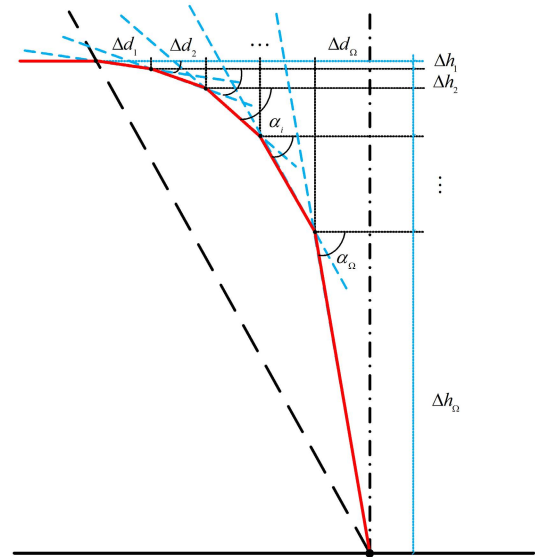


FIGURE 4. The approach angle scheduling algorithm used to avoid the target-loss situations in the autonomous quadcopter precision landing onto a ground moving target.

- Else, jump to *Step 4*.
- Step 6:* If the vehicle and the LT are vertically close, final approach the LT's surface.
Else, jump to *Step 7*.
- Step 7:* If the vehicle has used the maximum attempts of target search, jump to *Step 8*.
Else, climb to the predefined LT searching altitude.
- Step 8:* If the landing target is visible, jump to *Step 3*. Else, land at its current position.
- Step 9:* If the quadcopter is fully landed, landing complete.
Else, jump to *Step 8*.
- Step 10:* Finish.

The flowchart in Figure 5 illustrates the above procedure. Additionally, the steps from *Step 3* through *Step 6* can be described in more detail as follows.

Once the camera detects the LT, the planner will instruct the quadcopter to reduce its current altitude by a specific amount while horizontally approaching the LT, i.e., the quadcopter is commanded to pass through several discrete altitude setpoints until the landing task completes. If we let N be the number of discrete setpoints, i the current step among the N steps of setpoint changes (Figure 4), α_i the so-called approach angle, i.e., the angle between the horizontal plane and a vector pointing toward the ground (these angles are chosen by trial and error), Δd_i and Δh_i ($i = 1 \dots N$) the horizontal and vertical displacements from the vehicle's current position to its next setpoint, respectively, then Δh_i is calculated as:

$$\Delta h_i = \Delta d_i \tan \alpha_i \quad (26)$$

Then, the desired altitude corresponding to the i th step, $z_{sp|i}$, is determined as

$$z_{sp|i} = z_{sp|i-1} - \Delta h_i \quad (27)$$

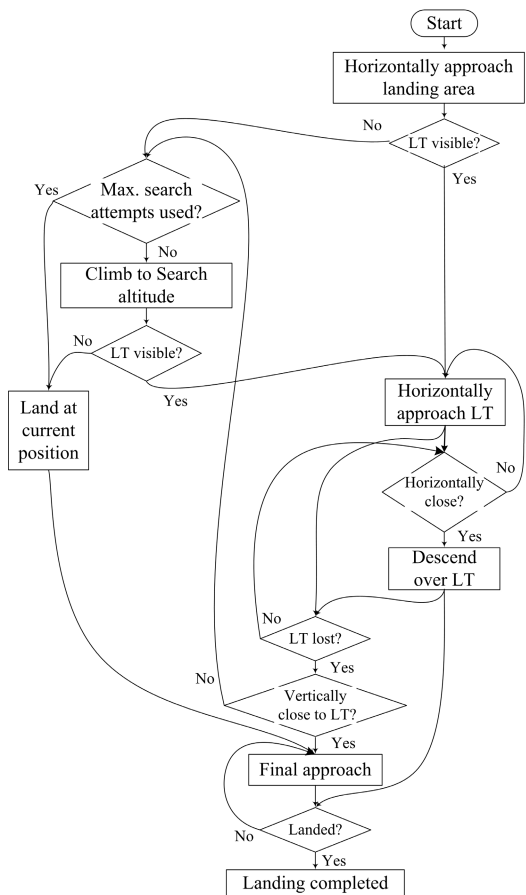


FIGURE 5. The flowchart illustrating the proposed autonomous landing procedure target.

IV. SIMULATION AND EXPERIMENT RESULTS

A. SIMULATION RESULTS

We first ran numerical simulations in Matlab/Simulink to verify the proposed DOB controller before applying our approach to a real-world quadcopter system. The numerical simulation was conducted based on the following assumptions. The quadrotor altitude, attitude, and the corresponding rates are measured by appropriate sensors and fed back to the DOB controller. The vehicle’s dynamics (4), the controller (15), and the disturbance observer (17) are implemented in Matlab/Simulink and operated at a sampling time of 0.0025 seconds, corresponding to a frequency of 400 Hz. The dynamical parameters are collected based on our experimental quadcopter’s specifications (Table 2). The controller and observer gains are listed in Table 3. The disturbance influencing the dynamics is introduced as:

$$d = \begin{bmatrix} 0.5\sin(0.8\pi t) \\ 0.2\sin(2\pi t) \\ 0.2\sin(2\pi t + \pi/3) \\ 0.2\sin(2\pi t - \pi/12) \end{bmatrix} + w_d \quad (28)$$

with w_d being the vector of four white noise elements.

TABLE 2. The parameters of the quadcopter dynamics.

Parameter	Value	Unit
m	2.68	kg
J_x, J_y, J_z	0.0175, 0.0140, 0.0223	kg.m ²
L	0.225	m
g	9.81	m/s ²

TABLE 3. The controller and observer gains.

Symbol	Value and Unit	Description
K	diag(10.48, 9.65, 9.65, 8.8)	Controller gain
Λ	diag(0.82, 1.15, 1.15, 1.05)	Controller gain
Γ	diag(9.0, 11.0, 11.0, 10.5)	Observer gain

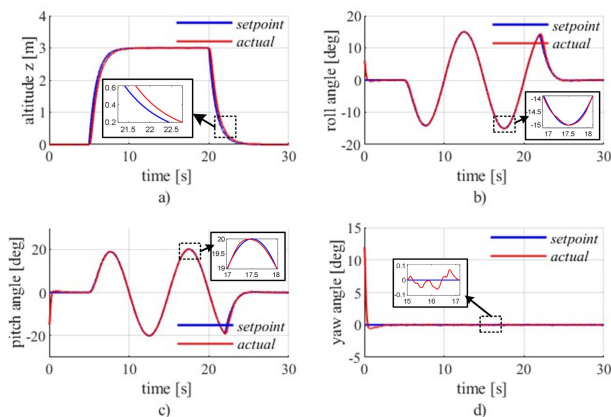


FIGURE 6. The altitude (a) and attitude (b)–(d) tracking performance in the numerical simulation.

The simulation scenario can be described as follows. At $t = 0$ s, the quadcopter is armed on a level surface at an altitude $z = 0$ m. At $t = 5$ s, the vehicle takes off and begins to ascend to the desired altitude of 3 m (Figure 6). At the same time, the quadcopter starts tracking the time-varying attitude setpoints:

$$\phi_{sp} = \frac{\pi}{12}\sin(0.2t); \quad \theta_{sp} = \frac{\pi}{9}\cos(0.2t + \frac{\pi}{2}); \quad \psi_{sp} = 0; \quad (29)$$

At $t = 20$ s, while tracking the attitude references, the vehicle is commanded to land.

It can be seen in Figures 6 through 8 that the entire algorithm, including the disturbance observer and the DOB controller, delivers superior stable and robust performance. As per the insets in Figure 6, the altitude command is tracked with a tracking delay of fewer than 0.25 seconds, and the attitude tracking performance is also superior with negligible tracking delays and errors (less than 0.05 seconds and 0.2 degrees, respectively). Furthermore, the control inputs are stable and do not exhibit any chattering (Figure 7). The disturbance observer also provides stable and reliable estimations (Figure 8), which has a time delay of fewer than 0.1 seconds and an average error of less than 7%. These simulation results provide a convincing numerical verification

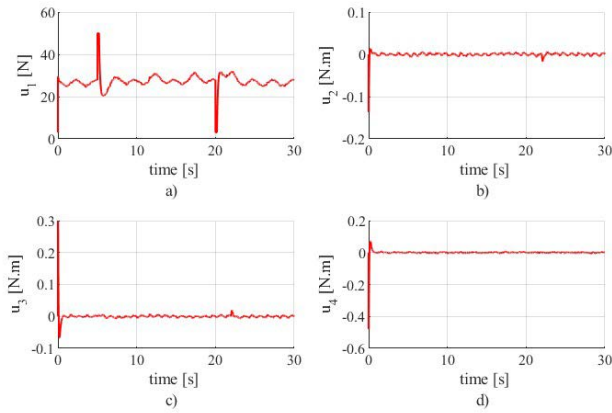


FIGURE 7. The robust control input performance of the proposed DOB controller in the numerical simulation. (a) u_1 ; (b) u_2 ; (c) u_3 ; (d) u_4 .

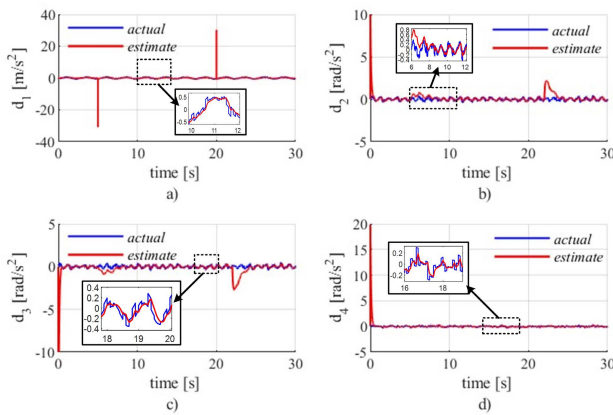


FIGURE 8. The disturbance estimation performance of the proposed disturbance observer in the numerical simulation. (a) d_1 ; (b) d_2 ; (c) d_3 ; (d) d_4 .

of the stability and feasibility of our DOB control algorithm for quadcopter systems. However, despite these encouraging theoretical results, we still need to test the performance of our approach on an experimental platform in real flight environments.

B. EXPERIMENTAL SETUP

1) EXPERIMENTAL QUADCOPTER PLATFORM

The quadcopter used in the experiment (Figure 9) is operated by an onboard computer Pixhawk FCU. A light detecting and ranging sensor LidarLite V3 is used to provide the altitude information while a commercial GPS receiver is used for positioning. The vehicle is also equipped with an inertial navigation system (INS) for its attitude and acceleration determination purposes. In addition, a Li-Po battery and a power regulator for power supply, a set of radio frequency transmitter/receiver for manual control, and a pair of wireless telemetry for ground station monitoring are utilized. We use an IR Pixy camera [36] to detect the landing platform and determine its position. The measurement is updated at a frequency of 50 Hz. Besides, an Odroid XU4 [37] serves as a companion computer to execute the proposed algorithms

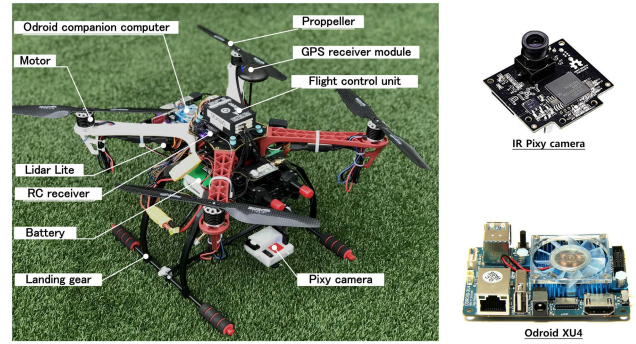


FIGURE 9. The experimental quadcopter platform and its equipped devices.

TABLE 4. Parameters of the ground moving vehicle.

Parameter	Value	Unit
L x W x H	0.95 x 0.75 x 0.2	m
L_r	0.25	m
Max. speed	2.0	m/s
Max. payload	5.0	kg
Power supply	14.8 – 17.4	V

(Figure 10). The Odroid XU4 and Pixhawk FCU exchange data through the Mavlink protocol. All relevant quadcopter dynamic parameters are listed in Table 2.

2) GROUND MOVING TARGET

The horizontally mobile platform simulates a UAV landing pad placed on ground vehicles like a car. It is constructed by a wooden plate attached to the top of a rover (Figure 11). The rover is equipped with a radio receiver and 4-cell Lithium battery and can be controlled remotely through a radio transmitter. A wheel-gear is attached at each corner of the wooden plate supporting the pad in case the quadcopter approaches the pad at its corners. The IR beacon is located at the center of the plate and shares the power supply system with the rover. The detailed parameters of this platform are listed in Table 4.

From the practical point of view, the landing platform may move along various kinds of trajectories. Nevertheless, in the most popular applications, such as disaster monitoring, surveillance, and search and rescue, the landing targets move in large areas, and their trajectories can be approximately considered successive straight lines. Therefore, we implemented the same directed movement in our rover. Due to the limited size of our flight test site, we could only choose the moving target with maximum speed of 2 m/s. Perceiving that this is not a large speed, we let the rover’s speed continuously varies in the range close to 2 m/s to have a fast enough movement of the landing target.

3) SOFTWARE

The proposed DOB controller is implemented on the Pixhawk FCU at 400 Hz, while our autonomous landing planner operates on the Odroid XU4 at 100 Hz (see Figure 10 which also includes other important elements of the control

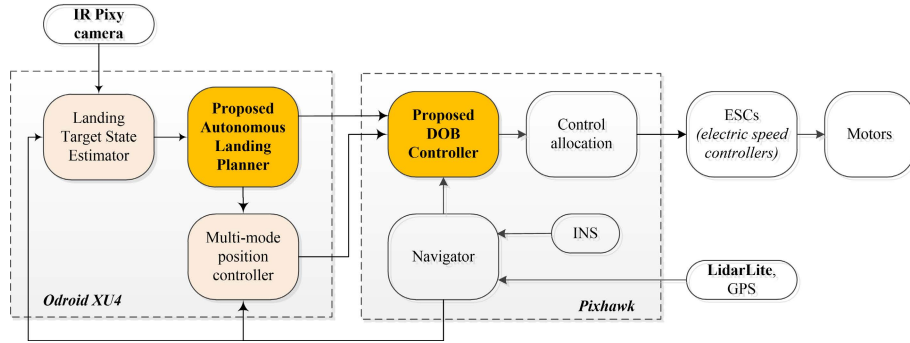


FIGURE 10. Block diagram of the system signal flow (the orange-colored blocks indicate the proposed algorithms).

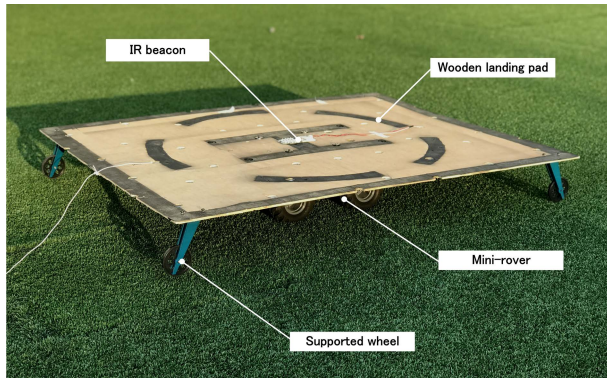


FIGURE 11. The ground moving platform (a rover) used in this study.

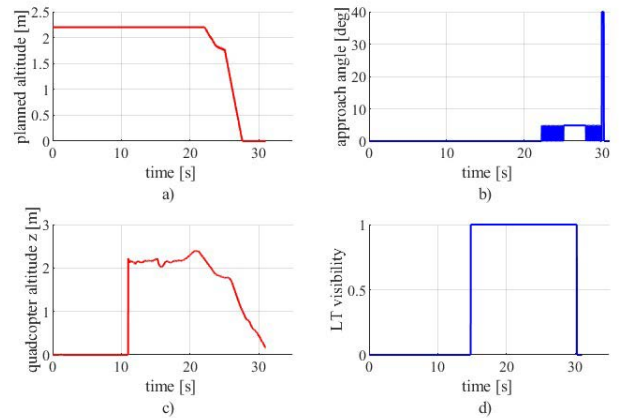


FIGURE 13. Performance of the planned altitude setpoint (a) approach angle (b), quadcopter’s altitude (c), and landing target (LT) visibility (d) when the quadcopter is exhibiting the landing mission over a ground moving target (rover).

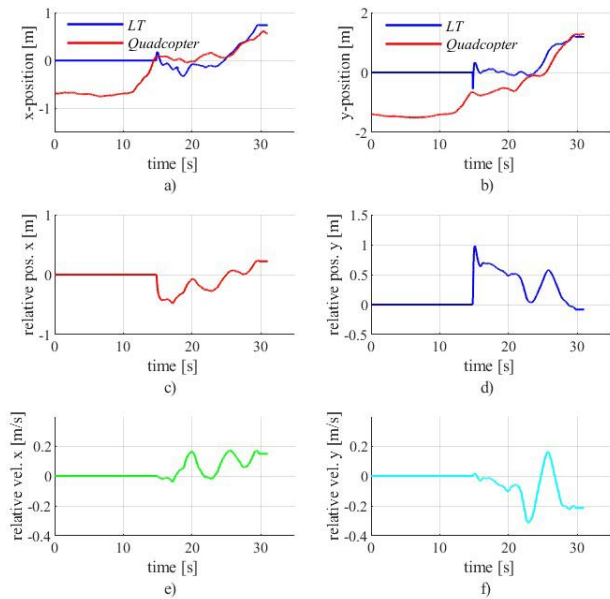


FIGURE 12. Landing target approaching control performance, including (a, b) the positions of the quadcopter and landing target (LT) in {E}, and (c, d) their relative position and (e, f) their relative velocity in {B}.

system). For the experiments, we used the simulation-verified observer and DOB controller gains from Table 3, tuning them

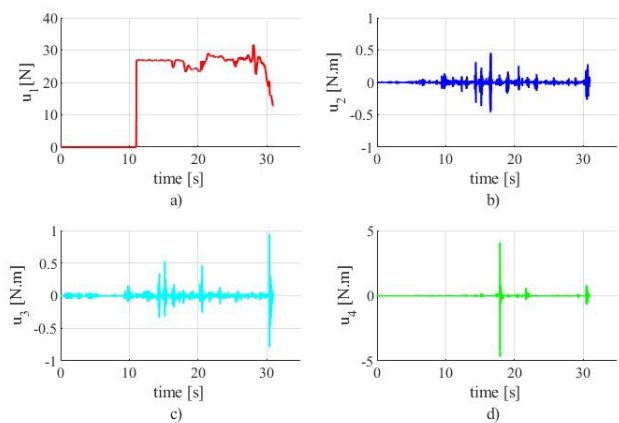


FIGURE 14. The control input performance, u_i ($i = 1 \dots 4$), while it is exhibiting the landing mission over a ground moving target (rover). (a) u_1 ; (b) u_2 ; (c) u_3 ; (d) u_4 .

only slightly. It is worth noting that for the quadcopter to track and land precisely on the moving target, its horizontal position (relative to the target) needs to be known fairly precisely which requires a position controller that can deliver the required level of precision. To that end, we used our

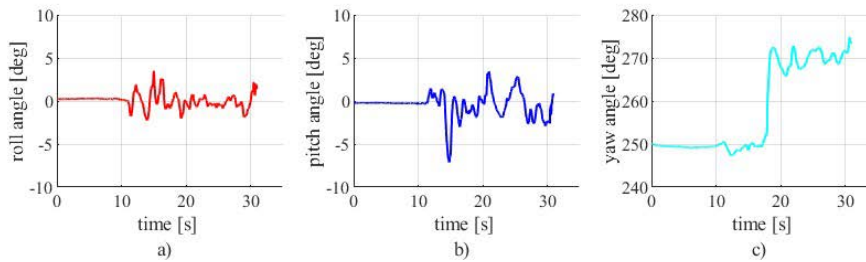


FIGURE 15. The quadcopter attitude performance while it is exhibiting the landing mission over a ground moving target (rover). (a) roll angle; (b) pitch angle; (c) yaw angle.

previously published vision-based landing target state estimator [31] and our multi-mode control technique [38], which have both been verified experimentally (see [31] and [38] for detailed descriptions of these algorithms).

C. EXPERIMENTAL RESULTS AND DISCUSSIONS

In this experiment we intended to test the tracking and landing performance of the quadcopter with a ground moving target (rover) using the following scenario: (1) the vehicle takes off and climbs to an altitude of 2.2 m above the test site floor; (2) the vehicle horizontally approaches the moving landing platform; (3) once the LT is detected by the IR camera, the landing task is triggered.

Once the LT has been detected (at $t \approx 11$ s), the quadcopter's performance (Figures 12 through 14) can be seen as consisting of two stages: (i) LT tracking; and (ii) LT approaching and landing. The first stage is from $t \approx 11$ to $t \approx 22$ s. As long as the distance to the target remains large (> 0.3 m), the planner maintains the UAV at the 2.2 m altitude setpoint (Figure 13a), and the approach angle remains zero (Figure 13b). The UAV thus only tracks the landing target (Figures 12a and 12b) while maintaining a constant altitude (Figure 13c). During this stage, the position controller is trying to manipulate the quadcopter closer to the LT in order to reduce their horizontal distance. It can be seen in Figure 13c that, at $t \approx 15$ s, the feedback altitude saw a declination of 0.2 meters as the UAV started to be directly above the 0.2-meter-high landing platform, thereby shortening the distance measured by the ranging sensor (the attached LidarLite).

Once the horizontal distance has been reduced to < 0.3 m ($t \approx 11$ s), the approach angle starts to change and the altitude setpoints are starting to decrease as the UAV initiates the landing procedure. In response to these commands, the DOB controller lowers the vehicle's altitude until the landing task is completed (Figure 13c) while the position controller maintains the horizontal tracking of the target (Figures 12a and 12b). However, the planned approach angle occasionally returns to zero and the altitude setpoint to 2.2 m (Figure 13b) indicating that the approach is not smooth throughout. These changes are due to the fact that the landing target and quadcopter are both in motion and as their relative horizontal distance is close to the limit that initiates the landing procedure (0.3 m), the UAV may change back and forth between

TABLE 5. Landing accuracy over several experiments of the autonomous quadcopter precision landing onto a ground moving target.

Criteria /	Flight	1	2	3	4	5	Average
x error (cm)		12	18	10	8	13	12.2
y error (cm)		10	12	20	15	10	13.4
$x - y$ error (cm)		16	22	22	17	16	18.6

a purely tracking and landing mode. Once the final landing procedure has been initiated (at $t \approx 22$), the landing mission completes within about 10 s and an accuracy of 16 cm. Both the attitude (Figure 15) and the control input performance (Figure 14) confirm the stability and effectiveness of the proposed method.

In order to verify the reliability of our algorithms, we conducted five additional experiments, two of which at night, with results shown in Table 5. As per this table, the best landing accuracy reaches 8 cm and 10 cm along the x and y axes, respectively. In the $x - y$ plane, the landing accuracy varied from 16 cm to 22 cm with an average of 18.6 cm. These values demonstrate the stability and reliability of the proposed method under real-world flight conditions. Furthermore, these encouraging results indicate that quadcopter UAVs may be suitable for use in many new real-world applications.

V. CONCLUSION

This paper presented a landing solution for a quadcopter to land precisely on a ground moving target. The successful landing experiments clearly demonstrated the effectiveness, reliability, and applicability of our work. The proposed DOB controller enables the quadcopter's ability to exhibit the landing missions stably and rapidly in actual flight conditions where the vehicle is always considerably influenced by many kinds of external disturbances. The landing planner allows the mission to be conducted automatically in a safe and reliable manner. Our method is extensible and can be directly used in real-world applications that require moving target landing. We dedicate our future work to a solution enabling quadcopter precision landing on a three-dimensional, i.e., horizontally and vertically, moving target.

REFERENCES

- [1] M. Idrissi, M. Salami, and F. Annaz, "A review of quadrotor unmanned aerial vehicles: Applications, architectural design and control algorithms," *J. Intell. Robot. Syst.*, vol. 104, no. 2, pp. 1–33, Feb. 2022.
- [2] V. Chamola, P. Kotesch, A. Agarwal, Naren, N. Gupta, and M. Guizani, "A comprehensive review of unmanned aerial vehicle attacks and neutralization techniques," *Ad Hoc Netw.*, vol. 111, Feb. 2021, Art. no. 102324.
- [3] N. X. Mung, N. P. Nguyen, D. B. Pham, N. N. Dao, and S. K. Hong, "Synthesized landing strategy for quadcopter to land precisely on a vertically moving apron," *Mathematics*, vol. 10, no. 8, p. 1328, Apr. 2022.
- [4] W. Liu, Z. Li, S. Sun, M. K. Gupta, H. Du, R. Malekian, M. A. Sotelo, and W. Li, "Design a novel target to improve positioning accuracy of autonomous vehicular navigation system in GPS denied environments," *IEEE Trans. Ind. Informat.*, vol. 17, no. 11, pp. 7575–7588, Nov. 2021.
- [5] S. A. S. Mohamed, M.-H. Haghbayan, T. Westerlund, J. Heikkonen, H. Tenhunen, and J. Plosila, "A survey on odometry for autonomous navigation systems," *IEEE Access*, vol. 7, pp. 97466–97486, 2019.
- [6] N. El-Sheimy and Y. Li, "Indoor navigation: State of the art and future trends," *Satell. Navigat.*, vol. 2, no. 1, pp. 1–23, 2021.
- [7] X. Zhang, B. Xian, B. Zhao, and Y. Zhang, "Autonomous flight control of a nano quadrotor helicopter in a GPS-denied environment using on-board vision," *IEEE Trans. Ind. Electron.*, vol. 62, no. 10, pp. 6392–6403, Oct. 2015.
- [8] H. Shi, G. Sun, Y. Wang, and K.-S. Hwang, "Adaptive image-based visual servoing with temporary loss of the visual signal," *IEEE Trans. Ind. Informat.*, vol. 15, no. 4, pp. 1956–1965, Apr. 2019.
- [9] X. Zhang, Y. Fang, X. Zhang, J. Jiang, and X. Chen, "Dynamic image-based output feedback control for visual servoing of multirotors," *IEEE Trans. Ind. Informat.*, vol. 16, no. 12, pp. 7624–7636, Dec. 2020.
- [10] H. W. Ho, G. C. H. E. de Croon, E. van Kampen, Q. P. Chu, and M. Mulder, "Adaptive gain control strategy for constant optical flow divergence landing," *IEEE Trans. Robot.*, vol. 34, no. 2, pp. 508–516, Apr. 2018.
- [11] T. Yang, P. Li, H. Zhang, J. Li, and Z. Li, "Monocular vision SLAM-based UAV autonomous landing in emergencies and unknown environments," *Electronics*, vol. 7, no. 5, p. 73, May 2018.
- [12] D. Cabecinhas, R. Naldi, C. Silvestre, R. Cunha, and L. Marconi, "Robust landing and sliding maneuver hybrid controller for a quadrotor vehicle," *IEEE Trans. Control Syst. Technol.*, vol. 24, no. 2, pp. 400–412, Mar. 2016.
- [13] V. M. Goncalves, R. McLaughlin, and G. A. S. Pereira, "Precise landing of autonomous aerial vehicles using vector fields," *IEEE Robot. Autom. Lett.*, vol. 5, no. 3, pp. 4337–4344, Jul. 2020.
- [14] J. Thomas, J. Welde, G. Loianno, K. Daniilidis, and V. Kumar, "Autonomous flight for detection, localization, and tracking of moving targets with a small quadrotor," *IEEE Robot. Autom. Lett.*, vol. 2, no. 3, pp. 1762–1769, Jul. 2017.
- [15] A. Borowczyk, D. T. Nguyen, A. P.-V. Nguyen, D. Q. Nguyen, D. Saussie, and L. J. Ny, "Autonomous landing of a multirotor micro air vehicle on a high velocity ground vehicle," *Satell. Navigat.*, vol. 50, no. 1, pp. 1–23, 2017.
- [16] J. Ghommam and M. Saad, "Autonomous landing of a quadrotor on a moving platform," *IEEE Trans. Aerosp. Electron. Syst.*, vol. 53, no. 3, pp. 1504–1519, Jun. 2017.
- [17] O. Araar, N. Aouf, and I. Vitanov, "Vision based autonomous landing of multirotor UAV on moving platform," *J. Intell. Robot. Syst.*, vol. 85, no. 2, pp. 369–384, Feb. 2017.
- [18] T. Baca, P. Stepan, V. Spurny, D. Hert, R. Penicka, M. Saska, J. Thomas, G. Loianno, and V. Kumar, "Autonomous landing on a moving vehicle with an unmanned aerial vehicle," *J. Field Robot.*, vol. 36, no. 5, pp. 874–891, Aug. 2019.
- [19] C. K. Tan, J. L. Wang, Y. C. Paw, and F. Liao, "Robust linear output feedback controller for autonomous landing of a quadrotor on a ship deck," *Int. J. Control*, vol. 92, no. 12, pp. 2791–2805, Dec. 2019.
- [20] A. Rodriguez-Ramos, C. Sampedro, H. Bavle, P. de la Puente, and P. Campoy, "A deep reinforcement learning strategy for UAV autonomous landing on a moving platform," *J. Intell. Robot. Syst.*, vol. 93, nos. 1–2, pp. 351–366, Feb. 2019.
- [21] Y. Huang, Z. Zheng, L. Sun, and M. Zhu, "Saturated adaptive sliding mode control for autonomous vessel landing of a quadrotor," *IET Control Theory Appl.*, vol. 12, no. 13, pp. 1830–1842, Sep. 2018.
- [22] Q. Lu, B. Ren, and S. Parameswaran, "Shipboard landing control enabled by an uncertainty and disturbance estimator," *J. Guid., Control, Dyn.*, vol. 41, no. 7, pp. 1502–1520, Jul. 2018.
- [23] L. Tan, J. Wu, X. Yang, and S. Song, "Research on optimal landing trajectory planning method between an UAV and a moving vessel," *Appl. Sci.*, vol. 9, no. 18, p. 3708, Sep. 2019.
- [24] Y. Chen, G. Zhang, Y. Zhuang, and H. Hu, "Autonomous flight control for multi-rotor UAVs flying at low altitude," *IEEE Access*, vol. 7, pp. 42614–42625, 2019.
- [25] X. Kan, J. Thomas, H. Teng, H. G. Tanner, V. Kumar, and K. Karydis, "Analysis of ground effect for small-scale UAVs in forward flight," *IEEE Robot. Autom. Lett.*, vol. 4, no. 4, pp. 3860–3867, Oct. 2019.
- [26] A. Gautam, M. Singh, P. B. Sujit, and S. Saripalli, "Autonomous quadcopter landing on a moving target," *Sensors*, vol. 22, no. 3, p. 1116, Feb. 2022.
- [27] J. Kwak, S. Lee, J. Baek, and B. Chu, "Autonomous UAV target tracking and safe landing on a leveling mobile platform," *Int. J. Precis. Eng. Manuf.*, vol. 23, no. 3, pp. 305–317, Mar. 2022.
- [28] J. Lin, Y. Wang, Z. Miao, H. Zhong, and R. Fierro, "Low-complexity control for vision-based landing of quadrotor UAV on unknown moving platform," *IEEE Trans. Ind. Informat.*, vol. 18, no. 8, pp. 5348–5358, Aug. 2021.
- [29] N. Xuan-Mung and S. K. Hong, "Robust backstepping trajectory tracking control of a quadrotor with input saturation via extended state observer," *Appl. Sci.*, vol. 9, no. 23, p. 5184, Nov. 2019.
- [30] J.-W. Lee, N. Xuan-Mung, N. P. Nguyen, and S. K. Hong, "Adaptive altitude flight control of quadcopter under ground effect and time-varying load: Theory and experiments," *J. Vibrat. Control*, vol. 2021, Oct. 2021, Art. no. 107754632110501.
- [31] N. Xuan-Mung, S. K. Hong, N. P. Nguyen, L. N. N. T. Ha, and T.-L. Le, "Autonomous quadcopter precision landing onto a heaving platform: New method and experiment," *IEEE Access*, vol. 8, pp. 167192–167202, 2020.
- [32] R. Pepy, A. Lambert, and H. Mounier, "Path planning using a dynamic vehicle model," in *Proc. 2nd Int. Conf. Inf. Commun. Technol.*, Apr. 2006, pp. 781–786.
- [33] K. D. Do and J. Pan, "Nonlinear control of an active heave compensation system," *Ocean Eng.*, vol. 35, nos. 5–6, pp. 558–571, Apr. 2008.
- [34] X. Liang, D. Wang, and S. S. Ge, "Continuous predictive control based on dynamic surface design with application to trajectory tracking," *Appl. Ocean Res.*, vol. 111, Jun. 2021, Art. no. 102615.
- [35] H. Khalil, *Nonlinear Systems*, 3rd ed. Upper Saddle River, NJ, USA: Prentice-Hall, 2002.
- [36] *CMUcam5 Pixy*. Accessed: 2022. [Online]. Available: <http://www.cmuacam.org/projects/cmuacam5>
- [37] *ODROID-XU4 User Manual*. Accessed: 2022. [Online]. Available: <https://magazine.odroid.com/wp-content/uploads/odroid-xu4-user-manual.pdf>
- [38] N. Xuan-Mung and S.-K. Hong, "Improved altitude control algorithm for quadcopter unmanned aerial vehicles," *Appl. Sci.*, vol. 9, no. 10, p. 2122, May 2019.



NGUYEN XUAN-MUNG (Member, IEEE)

received the B.S. degree in mechatronics from the Hanoi University of Science and Technology, Hanoi, Vietnam, in 2014, and the M.S. and Ph.D. degrees in aerospace engineering from Sejong University, Seoul, South Korea, in 2017 and 2021, respectively. From 2014 to 2015, he was with Samsung Electronics Vietnam Company Ltd., Vietnam. He is currently an Assistant Professor with the Department of Aerospace Engineering,

Sejong University. His research interests include unmanned aerial vehicles, control systems, automation, and robotics. He is also a Guest Editor of *Symmetry*.



fault-tolerant control, nonlinear control, intelligent control, and formation control.

NGOC PHI NGUYEN received the B.S. degree in mechatronics engineering from the HCMC University of Technology and Education, in 2012, the M.S. degree in mechatronics engineering from Vietnamese-German University, Vietnam, in 2015, and the Ph.D. degree in aerospace engineering from Sejong University, Seoul, South Korea, in 2020. He is currently an Assistant Professor with the Department of Aerospace Engineering, Sejong University. His research interests include



TAN NGUYEN received the M.E. and Ph.D. degrees from the Ho Chi Minh City University of Technology, Vietnam. He is currently a Lecturer at the Department of Technology, Dong Nai Technology University, Vietnam. His research interests include solving practice problems in structural engineering, artificial intelligence, and aerospace engineering.



research interests include robotics, dynamics, and applied nonlinear control.

DINH BA PHAM received the B.S. and M.S. degrees in mechanical engineering from Vietnam Maritime University, Hai Phong, Vietnam, in 2007 and 2012, respectively, and the Ph.D. degree in mechanical engineering from Kyung Hee University, Yongin, South Korea, in 2018. Since 2007, he has been with Vietnam Maritime University. He worked as a Postdoctoral Researcher in mechanical engineering at Sejong University, Seoul, South Korea, from 2019 to 2020. His



underwater vehicles and robotics, multi-body dynamic modeling, linear and nonlinear control, trajectory tracking, path planning, obstacle avoidance, and intelligent navigation.

MAI THE VU received the B.S. degree in naval architecture and marine engineering from the Ho Chi Minh City University of Technology, Vietnam, in 2013, and the Ph.D. degree from the Department of Convergence Study on the Ocean Science and Technology, Korea Maritime and Ocean University, South Korea, in 2019. He is currently an Assistant Professor at the Department of Unmanned Vehicle Engineering, Sejong University, South Korea. His research interests include



he was an Assistant Professor of intelligent mechatronics engineering with SJ. He is currently a Lecturer with the Mechatronics Department, Faculty of Mechanical Engineering, HCMUTE. His research interests include nonlinear control, sliding mode control, adaptive control, UAV flight control systems, mechatronics, and robotics. He received an Outstanding Research Award for his Ph.D. degree. He has been serving as a Guest Editor for *Sensor* journal (MDPI) and *Applied Sciences* journal (MDPI).

HA LE NHU NGOC THANH received the B.Sc. degree in automation technology from the HCMC University of Technology and Education (HCMUTE), Ho Chi Minh City, Vietnam, in 2011, the M.Sc. degree in mechatronics engineering from the HCMC University of Technology (HCMUT), Vietnam, in 2015, and the Ph.D. degree in mechanical and aerospace engineering from Sejong University (SJ), Seoul, South Korea, in 2019. From March 2019 to November 2020,



He is currently a Full Professor with the Department of Aerospace Engineering, Sejong University, South Korea. His research interests include fuzzy logic controls, inertial sensor applications, and flight control systems.

SUNG KYUNG HONG received the B.S. and M.S. degrees in mechanical engineering from Yonsei University, Seoul, South Korea, in 1987 and 1989, respectively, and the Ph.D. degree from Texas A&M University, College Station, TX, USA, in 1998. From 1989 to 2000, he was with the Flight Dynamics and Control Laboratory and the Unmanned Aerial Vehicle System Division, Agency for Defense Development, South Korea.

...